2.3 FORECASTING THE MAINTENANCE OF MESOSCALE CONVECTIVE SYSTEMS

Michael C. Coniglio[1,2], Melissa Bardon[3], Katrina Virts[4], and Steven J. Weiss[5]

[1]University of Oklahoma/Cooperative Institute for Mesoscale Meteorological Studies, Norman, Oklahoma
[2]NOAA/OAR/National Severe Storms Laboratory, Norman, Oklahoma
[3]School of Meteorology, University of Oklahoma, Norman, Oklahoma
[4]Department of Atmospheric Sciences, University of Washington, Seattle, Washington
[5]NOAA/NWS/Storm Prediction Center, Norman, Oklahoma

1. INTRODUCTION

Recent advances in numerical models and computing power have allowed for explicit real-time prediction of mesoscale convective systems (MCSs) over the past few years, some of which have supported field programs (Davis et al. 2004) and collaborative experiments at the Storm Prediction Center (SPC) (Kain et al. 2005). While these numerical forecasts are promising, their utility and how to best use the capabilities of the high-resolution models in support of operations is unclear (Kain et al. 2005). Therefore, refining our knowledge of the interactions of MCSs with their environment remains central to advancing our near-term ability to forecast MCSs.

a. MCS maintenance

The particular problem of forecasting how long an MCS will persist is fraught with challenges such as understanding how deep convection is sustained through system/environment interactions (Weisman and Rotunno 2004, Parker and Johnson 2004b, Coniglio et al. 2006a), how pre-existing mesoscale features influence the systems (Fritsch and Forbes 2001, Trier and Davis 2005), and how the system itself can alter the inflow environment and feed back to changes in the system structure and longevity (Parker and Johnson 2004b, Fovell et al. 2005).

Through the use of wind profiler observations and numerical model output, Gale et al. (2002) examine nocturnal MCSs to determine predictors of their dissipation. Similar to Evans and Doswell (2001), they find that changes in MCS speed may control its dissipation through changes in low-level storm-relative inflow. However, despite some indications that a decreasing low-level-jet intensity and low-level equivalent potential temperature and its advection can be useful in some cases, they did not find robust predictors of MCS dissipation, despite the importance of low-level shear in idealized numerical simulations.

An analysis of derecho proximity soundings in Coniglio et al. (2004) shows that significant wind shear often exists in mid and upper levels in the pre-convective environment. An emphasis of this work is that wind shear over deeper layers than those considered in past idealized modeling studies (Weisman and Rotunno 2004) may be important for MCS maintenance.

b. Goals

The goals of this work are to examine a large data set of observed proximity soundings to identify predictors of MCS dissipation and to improve our understanding of MCS environments in general. The ultimate goal is to develop a forecast tool that provides probabilistic guidance on the maintenance of MCSs. The focus is on the 3-12 hour time scale to benefit Day 1 Severe Weather Outlooks, Mesoscale Discussions, and the issuance of Severe Weather Watches at the SPC, and short-term forecasts issued by local National Weather Service forecast offices.

The intention is to examine the robust systems that obtain a linear or curved leading line (“quasi-linear”) and those that are driven primarily by cold pool processes and are not complicated by the presence of larger-scale external forcing (Fritsch and Forbes 2001, Trier and Davis 2005). The approach is to use statistical techniques to identify the best predictors of MCS dissipation and to use these predictors to develop an equation for the conditional probability of a strong, mature MCS. The best predictors of MCS dissipation are discussed in section 3. Section 4 introduces the MCS probability equation and illustrates its potential utility through some preliminary verification. A summary and final discussion are given in section 5.

2. DATA GATHERING AND PROCESSING

a. MCS proximity soundings

MCSs are identified by examining composites of base radar reflectivity for the months of May-August during the seven-year period of 1998-2004. MCSs that have a nearly contiguous quasi-linear or bowed leading edge of reflectivity values of at least 35 dbZ at least 100 km in length and that last at least 5 continuous hours are considered in this study.

From a set of over 600 MCSs of this type, we identified 269 events in which a radiosonde observation was taken within uncontaminated inflow no more than 200 km and 3 h away from the leading edge of the MCS. We added 79 derecho proximity soundings prior to 1998 that were identified using a similar procedure in Coniglio et al. (2004) to amass a set of 348 warm-season (May-August) MCS proximity soundings (Fig. 1).

At the time of the proximity sounding, the stage of the MCS in its lifecycle is defined as one of three stages: (1) initial cells prior to MCS development ("initiation"), (2) a mature MCS, with strengthening or quasi-steady high reflectivity (50 dBZ or higher) embedded within the nearly contiguous line of 35+ dbZ echoes ("mature"), and (3) a weakening MCS, with significantly weakened or shrinking areas of high reflectivity or a loss of system organization and associated areas of high reflectivity without any later re-intensification ("dissipation").

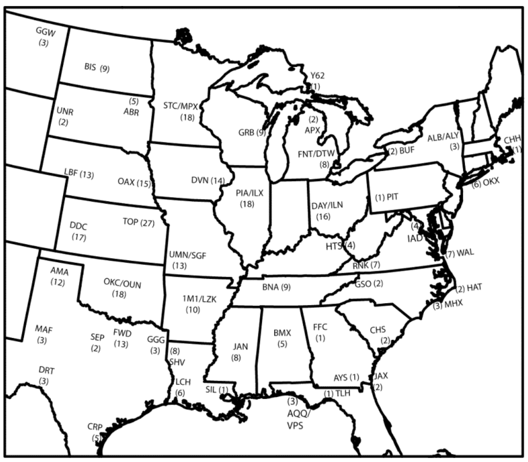

Fig. 1. The number and locations of soundings used in this study.

The predictors for MCS maintenance are then identified from a subset of 290 MCSs in which the leading line was moving ≥ 10 m s^{-1} near the sounding time to help remove the systems with significant back-building or quasi-stationary characteristics. These soundings are then stratified into 79 initiation, 96 mature, and 115 dissipation, soundings based on the appearance and trends of the radar reflectivity at the time of the sounding as described above.

b. Statistical Procedures

Several hundred variables were calculated from the soundings that represent various aspects of the kinematic and thermodynamic profile. We focus on a subset of variables that are found to have the largest statistically significant differences among the MCS categories (the "best predictors") while focusing on those variables that are often used by forecasters. The statistical procedure to identify the best discriminators and the development of the forecast tool involved a three-step procedure. First, the differences in variables between the mature and dissipation soundings are assessed using the Mann-Whitney significance test. Next, the variables that are found to be the most different are used as guidance in a linear discriminant analysis to find the number and particular combination of variables that best discriminate the mature and dissipation soundings. Finally, the variables found to best discriminate the mature and dissipation soundings are used as predictors to logistic regression, which creates an equation for calculating conditional probabilities of MCS maintenance. We refer the reader to Wilks (1995) and Coniglio et al. (2006b) for details on the components of this procedure.

3. BEST PREDICTORS

a. Mean wind shear

Although many of the differences of the wind shear variables (shear vector magnitudes, total shear, positive shear, etc.) between the mature and dissipation soundings are large, the greatest differences, as gauged by the Z-scores[1], are among the shear vector magnitudes (SVMs) over very deep layers (Fig. 2). Figure 2 is produced with forecasters in mind who often use SVMs as a primary component in predicting the mode and severity of convection.

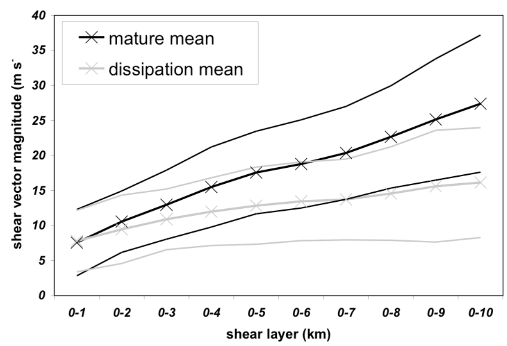

Fig. 2. Mean shear vector magnitudes (lines marked X) calculated over various depths among the mature (black) and dissipation (grey) sounding groups. The thin lines enclose +/- one standard deviation for the means.

These results suggest that if the SVM is used as a shear metric, then it is much better to look at deep layers versus shallow layers to forecast the weakening of MCSs. The differences in the low-level SVMs are relatively

[1] We use the property that significance of the differences between the two groups in the Mann-Whitney test is directly related to the magnitude of the Z-score (the larger the Z-score, the more significant the difference). For example, a Z-score of 1.96 (2.58) corresponds to a 95% (99%) confidence that the "locations" of the two distributions in space are different.

small, suggesting that these values, alone, have limited utility in determining the stage of the MCS lifecycle, as suggested for derechos by Evans and Doswell (2001) and Coniglio et al. (2004), and for MCSs in general by Gale et al. (2002) and Cohen et al. (2006). Indeed, the Z-scores for the deep-layer shear values are very large (5.0-8.0), whereas the Z-scores for the low-level shear values are much smaller (1.0-2.0) (not shown). In fact, the deep-layer SVMs have the largest Z-scores of *any* variables tested.

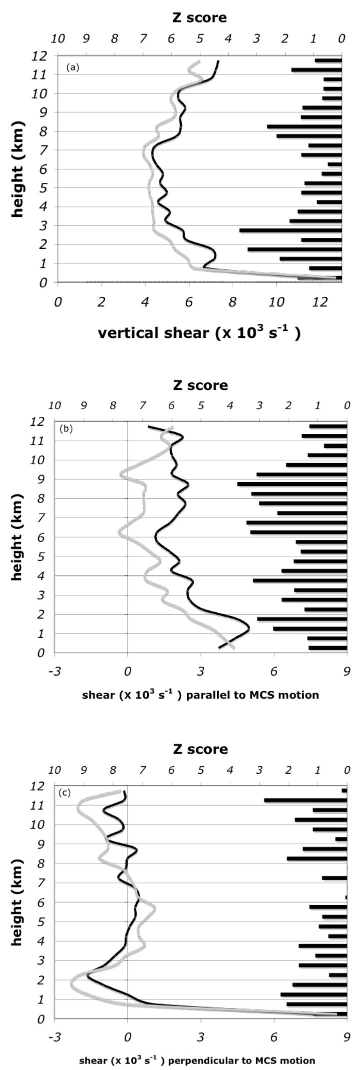

Fig. 3. (a) Mean shear profile calculated every 500 m for the mature (black line) and dissipation (grey line) soundings as a function of height AGL. The horizontal bars on the right side of the figure display the Z-score (using the x-axis at the top of the figure) for the differences in the shear between the mature and dissipation soundings at each vertical level. (b) as in (a) except for the mean shear profile parallel to the MCS motion vector (which is usually perpendicular to the MCS leading line). (c) as in (a) except for the mean shear profile perpendicular to the MCS motion vector.

A closer inspection of the shear profiles between the mature and dissipation soundings (Fig. 3) sheds light on the kinematic reasons for the difference in the SVMs. The overall shear profile ($\partial V_s(z)$ in units of s^{-1}) shows that the mean shear is greater for the mature soundings at every vertical level (Fig. 3a). Judging by the Z-scores on figure 3a, these differences are most significant between 2-3 km and near 8 km. Since Therefore, a measure that integrates these differences over a large depth should be beneficial versus a metric that only integrates over a shallow layer (low-level or upper-levels only), as revealed by the SVMs (Fig. 2) and total shear magnitudes (not shown).

An inspection of the shear components in MCS motion-relative coordinates helps elucidate how the shear is contributing to these differences (Figs. 3b&c). This is important to examine because the orientation of the shear and its vertical distribution plays a key role in the longevity and organizational characteristics of MCSs (Weisman et al. 1988, Parker and Johnson 2004c, Coniglio et al. 2006). It is clear that the mean component of the shear *parallel* to MCS motion ($\partial u_s(z)$), which is usually nearly perpendicular to the MCS leading line, is greater at all levels for the mature soundings, except very close to the ground and near the tropopause (Fig. 3b). Judging by the Z-scores on figure 3b, these differences are most significant at 1-2 km and at 6-9 km, in which the mean MCS motion-parallel shear for the mature soundings is nearly triple what it is for the dissipation soundings.

Looking at low-levels first, by viewing the mean component of shear *perpendicular* to MCS motion ($\partial v_s(z)$) (Fig. 3c), which is usually nearly parallel to the leading line, we see that the larger $\partial V_s(z)$ seen in the 1-2 km layer for the mature soundings (Fig. 3a) has a contribution from a larger positive $\partial u_s(z)$ for the mature soundings (Fig. 3b), but also has a contribution from a larger *negative* magnitude of $\partial v_s(z)$ for the dissipation soundings (Fig. 3c). The contributions from $\partial u_s(z)$ in the 1-2 km layer (Fig. 3b) are probably related physically to the organizational benefits of positive low-level line-perpendicular shear (Parker and Johnson 2004c, Weisman and Rotunno 2004). The reasons for the increase in negative line-parallel shear for the dissipation soundings isn't clear, but is likely related to a decrease in the southerly relative inflow component at 2-3 km (an inspection of these wind components verifies this claim). Collectively, figure 3 illustrates that the low-level SVMs represent differences in shear that are important in both the line-perpendicular and line-parallel directions.

Looking at upper-levels, the possible physical benefits to mature MCSs related to a larger upper-level shear component parallel to MCS motion (Parker and Johnson 2004a, Coniglio et al. 2006) are suggested on figure 3b. The larger overall shear vector in upper-levels (Fig. 3a) is almost entirely due to the larger $\partial u_s(z)$ (Fig. 3b) since $\partial v_s(z)$ is nearly identical at 6-8 km between the two groups (Fig. 3c).

Returning to the development of the forecast tool, it is desirable to define a shear predictor that accounts for the possibility of variable heights of the low-level or upper-level jets that can control the effective depth and magnitude of the deep-layer shear. Therefore, we define the "maximum deep shear" to be the maximum SVM between any wind vector in the lowest 1 km and any wind vector in the 6-10 km layer to be used in the logistic regression procedure. The Z-score for the maximum deep shear is slightly smaller than that for the 0-10 km shear, but still very large relative to the shallower shear.

b. Mean wind speeds

In addition to the deep-layer wind shear, the deep-layer mean wind speeds are very different between the mature and dissipation soundings. For example, the 3-12 km mean wind speed has the largest Z-score among the mean wind variables and is a large improvement over using a low-level only mean wind (e.g. 0-6 km). An examination of the mean wind speed profile (Fig. 4) reveals that the winds in upper levels contribute the most to this discrimination. Specifically, the mean wind speeds are greater for the mature soundings than the dissipation soundings at 99% confidence (Z > 2.65) at all levels above 5 km, and the confidence generally increases with height up to 12 km (Fig. 4). Inspection of the synoptic-scale flow patterns shows that this decrease in upper-level wind speeds for dissipating MCSs can usually be attributed in large part to the background flow in which the systems often propagate away from the upper-level features and associated jet streams that contributed to their initiation and maturity (Coniglio et al. 2004) (this also applies to decreases in upper-level shear as MCSs dissipate).

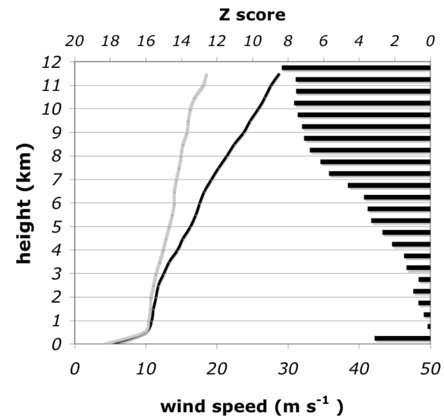

Fig. 4. As in fig. 3a, except for the mean wind speed.

c. Thermodynamic variables

Using similar procedures as described above, we examine many thermodynamic variables related to instability including, but not limited to, several variations of CAPE and lapse rates over many layers. We find that the mean lapse rates over a deep portion of the convective cloud layer (generally from the lifting condensation level to some level in the 500 hPa to 300 hPa layer) are the most different between the mature and dissipation soundings among the thermodynamic variables. Although it is not surprising that larger lapse rates are found for stronger, more mature MCSs, the physical importance of the deeper mid-level lapse rates versus the lower-level lapse rates is not obvious. One hypothesis is that steeper mid-level lapse rates make it easier for the shear in the convective cloud layer to maintain upright trajectories by allowing the convective updrafts to reach their vertical velocity potential earlier in the overturning process, as related to the processes described in Parker and Johnson (2004a) and Coniglio et al. (2006a). This could lead to more cells that unload their precipitation close to the leading edge of the gust front compared to systems that occur in a smaller mid-level lapse rate environment. The 3-8 km lapse rate has the highest Z-score among the two groups and is much better than using a low-level only lapse rate (e.g. 1-4 km), and is thus used as the primary instability variable in the logistic regression procedure.

Among the other thermodynamic variables, we find that various CAPEs that are based on finding the most unstable mixed parcel over some layer tend to have large Z-scores between the mature and dissipation soundings and, interestingly, are only weakly correlated with the 3-8 km lapse rates, as similarly shown by Blanchard (1998). The lack of a strong correlation appears to be because the CAPE variables are determined largely by the absolute moisture content in the layer with the maximum θ_e rather than the vertical temperature profile and its control on parcel buoyancy. As detailed next, the Rapid Update Cycle (RUC) (Benjamin et al. 2003) output is used to apply the results. Therefore, we use the method of calculating the "best" CAPE in the RUC model (hereafter denoted RCAPE) as another predictor in the logistic regression. In this method, if the parcel with the maximum θ_e is found in the lowest 70 h Pa, the RCAPE is calculated from a mixed parcel in the lowest 70 h Pa; otherwise, the single most-unstable parcel is used to calculate the CAPE (David Bright, personal communication).

d. Discriminant analysis

Although the number of variables that can be used in a linear discriminant analysis is unlimited theoretically, the results are best illustrated with a two-variable discrimination. In this data set, a linear discrimination using the 3-8 km lapse rate and the maximum deep shear separate 75% of the mature and dissipation soundings correctly (Fig. 5), which illustrates the potential utility of the deep shear and lapse rates in this context. Figure 5 clearly demonstrates that strong, mature MCSs generally persist in the larger deep shear, larger lapse rate portion of the parameter space and MCSs generally dissipate under the weaker deep shear, smaller lapse rate portion of the spectrum. However, several outliers are present that do not fit the overall pattern and it is instructive to briefly examine their characteristics.

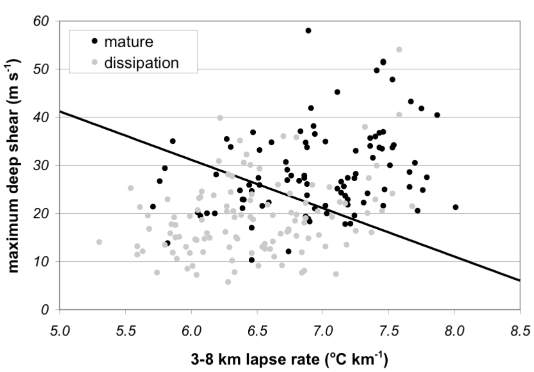

Fig. 5. Scatter plot of the maximum deep shear (m s^{-1}) versus the 3-8 km lapse rate (C km^{-1}) for the mature and dissipation soundings. The linear discrimination line separates 75% of the soundings correctly.

An examination of five of the mature soundings found in the lower left corner of figure 5 reveals recurring features, such as large surface-based CAPE (> 3500 J kg^{-1}), very high equilibrium levels (ELs) (14 to 16 km AGL), very little convective inhibition (CIN) in which the lifting condensation level (LCL) ≅ the level of free convection (LFC), and high relative humidity from the surface to 500 hPa. In addition, all but one case have very low lifting condensation levels (LCLs) (~600 to 800 m) (the exception was a sounding from Dodge City, KS taken in a deep well-mixed boundary layer). In these environments, large parcel buoyancy (governed by the lapse rates) and shear apparently become unnecessary to retrigger and organize convection along the cold pool, or any other linear forcing mechanism, given the relative ease that parcels can rise nearly undiluted to the high EL.

A similar inspection of MCSs that dissipate despite large 3-8 km lapse rates and large maximum shear values (found in the upper right corner of figure 5) does not reveal obvious similarities among the outliers and potential reasons for the dissipation seem to vary from case to case. For example, the obvious outlier with a lapse rate ≈ 7.6 K km^{-1} and shear ≈ 54 m s^{-1} occurred on May 2 under unseasonably strong synoptic scale forcing and the dissipation was coincident with the squall line outrunning the strong frontal convergence. Another system had its inflow contaminated by a cold pool remaining from a mesoscale region of light rain from earlier in the day shortly after the sounding was taken. In another case, the system became oriented parallel to the shear precluding the further organization of a progressive linear system. Therefore, while MCSs that persist despite small lapse rates and deep shear may perhaps be identifiable by the vertical distribution of the thermodynamic properties of the sounding, it is not as obvious that dissipating MCSs in large lapse rates and deep shear can be anticipated as easily and is a limitation of this approach.

A small improvement to the discrimination is found when the RCAPE and the 3-12 km men wind speed are used in the discrimination, along with the maximum deep shear and the 3-8 km lapse rate. These four variables collectively separate over 80% of the mature and dissipation soundings correctly. It is worth noting that, because of the mutual correlations among the hundreds of variables, any additional variables provide negligible (< 1%) improvement to the discrimination of the two groups. Therefore, the maximum deep shear (*maxshear*), 3-8 km lapse rate (*3-8 lr*), RCAPE, and 3-12 km mean wind (*3-12 mw*) are used as input to the logistic regression procedure, which is described next.

4. APPLICATIONS AND EVALUATION

a. MCS Maintenance Probability (MMP)

The logistic regression procedure described in Wilks (1995) and executed in the Splus 6.1

software package is used to develop the MCS maintenance probability (MMP) equation:

$$\underline{\underline{For\ RCAPE \geq 100\ J\,Kg^{-1}}}:$$

$$MMP = \frac{1}{\left[1 + EXP\left(a_0 + (a_1 * \{\max shear\}) + (a_2 * \{3-8\ lr\}) + (a_3 * \{RCAPE\}) + (a_4 * \{3-12\ mw\})\right)\right]} \quad (1)$$

$$\underline{\underline{For\ RCAPE < 100\ J\,Kg^{-1}}}:$$

$$MMP = 0,$$

where the regression coefficients are a_0 = 13.0 (dimensionless), a_1 = -4.59 x 10^{-2} m^{-1} s, a_2 = -1.16 C^{-1} km, a_3 = -6.17 x 10^{-4} J^{-1} kg, and a_4 = -0.17 m^{-1} s. Note that the MMP is set to zero for RCAPE values below 100 J kg^{-1} regardless of the values of the other predictors.

As illustrated in figure 6, if all four of the predictors obtain their median values in the combined mature and dissipation sounding data set (*maxshear* = 21 m s^{-1}, *3-8lr* = 6.7 C^{-1} km, *RCAPE* = 1731 J kg^{-1}, *3-12mw* = 17 m s^{-1}), then the regression equation predicts an 85% chance[2] that the MCS will be strong and be maintained. In general, a steeper curve suggests a better ability to discriminate between the two groups and, therefore, the steepness of this curve (Fig. 6) suggests the potential for substantial skill in discriminating mature and weakening MCSs.

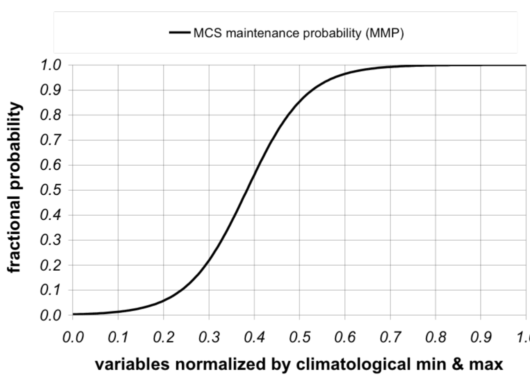

Fig. 6. Plot of eq. (1) for the predictors normalized by their minimum and maximum values in the data subset. For example, if all four of the predictors for the equation for MCS maintenance are exactly half way between their minimum and maximum values (0.5), then the regression equation predicts an 85% chance that the MCS will be strong and maintained. In dimensional values, this corresponds to a maximum deep shear of 21 m s^{-1}, a 3-8 km lapse rate of 6.7 C^{-1} km, a RCAPE of 1731 J kg^{-1}, and a 3-12 km mean wind speed of 17 m s^{-1}.

[2] Note that this is only one of many ways that a probability of 85% can be reached depending on the values of the predictors. For example, one particular sounding in the data set has *maxshear* = 42 m s^{-1}, *3-8lr* = 6.9 C km^{-1}, *RCAPE* = 383 J kg^{-1}, *3-12mw* = 21 m s^{-1}, and also has an MMP of 85%.

b. Preliminary evaluation of the MMP

As part of the NOAA/SPC/NSSL Hazardous Weather Testbed (http://www.nssl.noaa.gov/hwt), 45 MCSs that occurred during the months of June, July, and August in 2005 (Fig. 7) were documented to evaluate the MMP on an independent data set. For each event, documentation included traces of the system's leading edge at the top of each hour between its genesis and dissipation times. To evaluate the performance of the MMP, the first available RUC forecast cycle before the MCS genesis time was used to calculate the mean MMP value along the MCS trace line coincident with the hour of the RUC forecast. This estimation of a single MMP value along the entire leading edge was sometimes problematic, especially in cases where a portion of the MCS leading line stretched across a tight gradient of the probabilities. However, we focused on the values along the strongest and most organized portion of the system to define a representative value, which alleviated some ambiguity in many cases. In addition, if an MCS persisted beyond 12 hours, it was necessary to include parameter values calculated from two different RUC model initialization times since RUC forecasts are limited to 12 hours, which added some discontinuity to the evaluation.

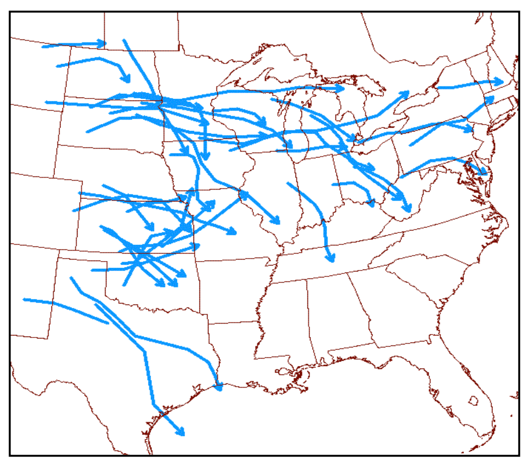

Fig. 7. Arrows indicating the location and direction of movement of the central portion of each MCS case in the independent evaluation data set.

The MCSs varied greatly in their longevity, varying from a minimum of 5 hours (as required by our MCS criteria) to over 24 hours. Since the goal is to characterize MMP values among a large number of MCS lifecycles, the total time of each MCS was normalized (i.e., t = 0 at MCS genesis, t = 0.5 exactly halfway through its lifetime, and t = 1 at the time of dissipation). It is

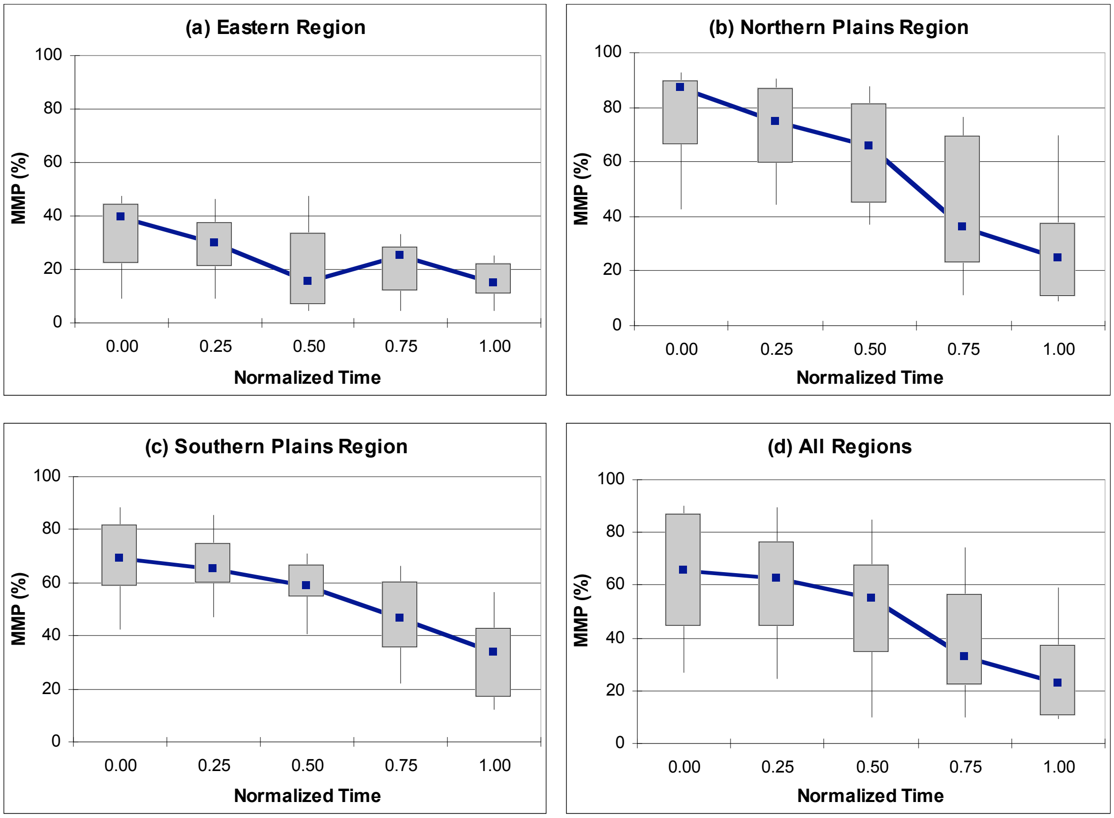

Fig. 8. Distribution of MMP plotted against normalized time for (a) Eastern, (b) Northern Plains, (c) Southern Plains, and (d) all MCS cases in the independent evaluation data set.

important to note, however, that it was common to observe MCSs that oscillated in intensity during their lifetime, especially for the long–lived systems. Therefore, a normalized time of 0.5 does not necessarily indicate that the MCS is at its maximum strength. Overall, however, the MCS was at its peak intensity at $t < 0.5$ and systems were typically undergoing steady weakening by $t > 0.75$.

Figure 8 displays the interquartile (IQ) (25^{th} to 75^{th} percentile) range of MMP values through the normalized MCS lifetimes for three geographic areas and for all cases combined. It is encouraging that the MMP overall shows a clear decreasing trend through the MCS lifetime and that the ranges show little to no overlap between the early and latter stages of the MCSs (Fig. 8d).

MMP behavior in the Northern and Southern Plains (Figs. 8b&c) is generally similar, with high initial values, which markedly decrease toward dissipation. Although the IQ range of MMP values for cases in the Northern Plains is fairly wide throughout MCS lifetime, there is a steep decrease in median MMP values with normalized time, particularly between t=0.50 and t=0.75 (Fig. 7b). This is a reflection of the frequent occurrence of a sharp gradient in the MMP from values > 70% to values < 30% as the MCSs begin their steady weakening.

Although the median MMP values for systems in the Southern Plains doesn't decrease as dramatically as those for the systems in the Northern Plains, the IQ range is smaller at all times, particularly during the middle portion of the MCS lifetime (t=0.5) (Fig. 8c). This is beneficial to forecasters because smaller IQ ranges allows for more confident prediction of MCS duration and suggests that a value of 50 to 60% can be used reliably to forecast the location where MCSs begin to weaken for good.

In contrast to the systems in the Plains sates, MMP values for the systems in the Eastern region are consistently lower and do not exhibit as steep of a decline with time as in the Plains regions (Fig. 8a). This behavior is likely in part due to the lower environmental input values, particularly lapse rates, typical of the eastern United States. This suggests that, although eastern U.S. MCS events were included in the developmental data set, the preponderance of events in the Midwestern and central U.S. leads to predictors that are most applicable to these regions and that some form of normalization or regionalization is required to apply the MMP equation to eastern U.S. events.

In summary, although the above evaluation is somewhat subjective and is limited by sample size, it does suggest that the MMP provides useful guidance on the transition of a system with a solid line of 50+ dbZ echoes to a more disorganized system with unsteady changes in structure and propagation characteristics. An example of how the MMP might be used effectively in a specific application is shown next.

c. Example of MMP application

On the evening of 30 June 2005, a nearly stationary synoptic front meandered from the Front Range of the Colorado Rockies southward into far northeastern New Mexico, then stretched eastward across the Texas Panhandle and eventually northeastward toward the central Mississippi River valley (Fig. 9). Isolated convection developed in east-central Colorado during the late afternoon and developed into an elevated supercell that moved through southeastern Colorado and southwestern Kansas from 0200 to 0500 UTC on 1 July (Fig. 9). Although northeasterly surface winds were found up to ~750 h Pa north of the front (not shown), the boundary layer was well-mixed and supported convectively generated surface winds > 40 m s^{-1}. The supercell then grew upscale and developed linear characteristics as it entered Oklahoma after 0600 UTC, with a continuation of the severe surface winds north of the front (Fig. 9).

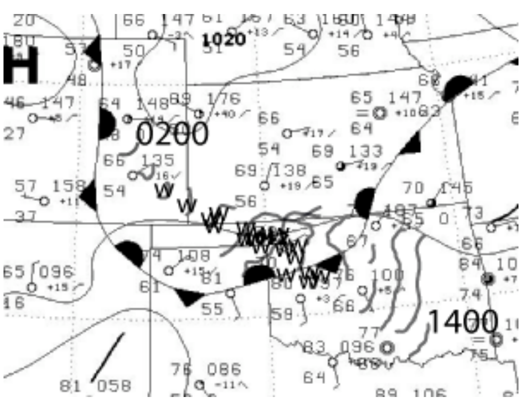

Fig. 9. Surface chart valid 0600 UTC on 1 July 2005 produced by the National Centers for Environmental Prediction. Solid grey lines denote the hourly positions of the leading edge of the 50+ dbz echoes associated with the supercell and MCS from 0200 UTC to 1400 UTC. "W" denotes the locations of severe wind reports.

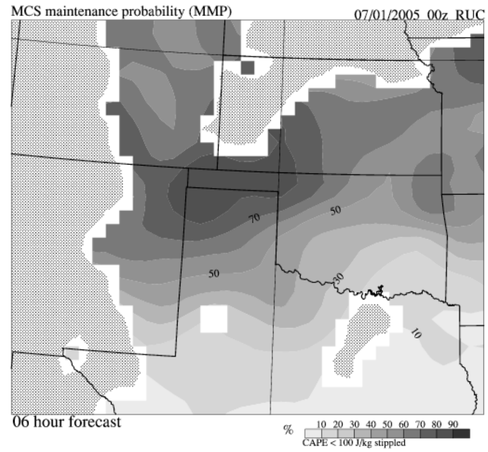

Fig. 10. MCS maintenance probabilities (MMP) (%) based on a 6-h RUC forecast valid at 0600 UTC 1 July 2005. Hatched areas represent areas with CAPE < 100 J kg^{-1}.

Although forecasters were aware of the potential for severe thunderstorm winds in this region, the persistence and strength of the thunderstorm winds north of the front were not anticipated. It is intriguing that the MMP values are high (> 70%) in the region that the supercell transitioned to an MCS in far southwestern Kansas and northwestern Oklahoma (Fig. 10).

By examining the components of the MMP (Fig. 11), it is evident that the maximum deep shear values of 70-80 kt and 3-8 km mean lapse rates over 7.5 K km^{-1} likely contributed most to the high probabilities, since the RCAPE values and the 3-12 km mean wind values are not particularly large (500–1500 J kg^{-1} and 35-40 kt, respectively). This could have steered forecasters to examine this area for the potential for organized severe surface winds more critically, despite the location of the system well north of the front in a region of northeasterly low-level flow.

Just as important, and perhaps the more challenging aspect of the forecast, was the cessation of the severe surface winds and the weakening of the convective system once it entered the warm sector air (Fig. 9), after which the line became more disorganized and propagated discretely. The line then reorganized temporarily into a solid but weaker linear system before dissipating altogether in eastern Oklahoma by 1400 UTC (Fig. 9). Just as the MMP could have increased the awareness of an organized severe wind threat in southwestern Kansas and far northwestern Oklahoma, the MMP values could have alerted forecasters to the rapidly decreasing probability of an organized system across central Oklahoma with values dropping quickly to 20-30% across this region (Fig. 10), despite the presence of an unstable and weakly-capped warm-sector airmass.

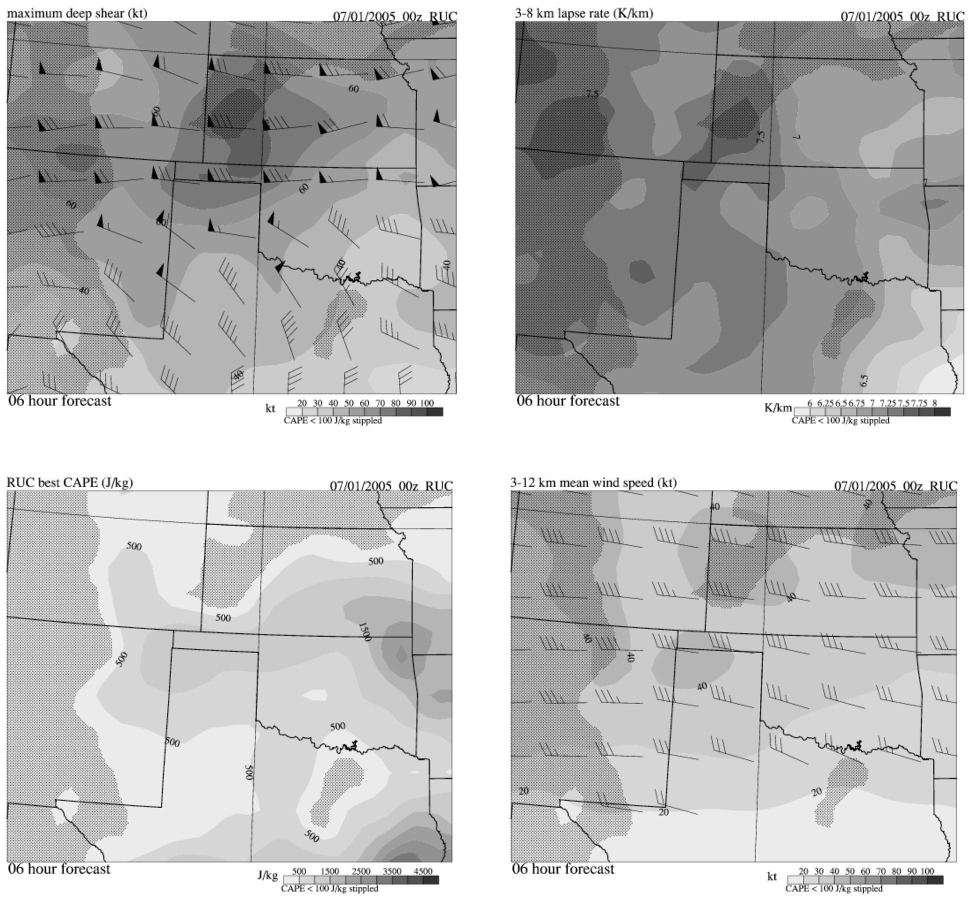

Fig. 11. Plots of the four components of the MMP, the maximum deep shear (kt), 3-8 km lapse rate (K km^{-1}), RUC "best" CAPE (J kg^{-1}), and 3-12 km mean wind (kt), based on a 6-h RUC forecast valid at 0600 UTC 1 July 2005. Hatched areas represent areas with CAPE < 100 J kg^{-1}.

Although the 3-8 km lapse rates, the CAPE and the 3-12 km mean wind speeds all show a decrease along the path of the system, a large gradient in maximum deep shear values that drop quickly from over 70 kt over the Oklahoma Panhandle to less than 40 kt across west-central Oklahoma (Fig. 11) appears to be the primary reason for the rapid drop in the MMP values.

5. SUMMARY AND DISCUSSION

This paper addresses the problem of predicting the maintenance of quasi-linear MCSs. Environmental variables that best differentiate between mature and weakening MCSs are identified from a large set of observed proximity soundings and are used to develop a tool that provides probabilistic guidance on MCS maintenance.

For the discrimination of mature and weakening MCS environments, the mean vertical wind shear over a very deep layer is found to be the variable with the largest statistical differences and is found to be a much better discriminator than the low-level-only shear variables. Mean lapse rates over a significant depth of the convective cloud, the maximum mixed-layer CAPE, and low-to-upper level mean wind speeds also discriminate between mature and weakening MCSs very well.

These results speak to the need for forecasters to look at the integration of sounding-derived parameters over a deep portion of the convective cloud layer in forecasting the near term behavior of quasi-linear MCSs and brings into question the utility of using low-level only parameters, including mean winds speeds, lapse rates, and the low-level vertical shear. Regarding the shear, the upper-levels of MCS environments has been given little attention in the literature compared to low-level shear (Weisman and Rotunno 2004), and we refer the reader to Parker and Johnson (2004b) and Coniglio et al. (2006 a&b) for a discussion on the physical importance of the deeper shears on MCS structure and longevity.

Early verification of the probabilistic forecast tool suggests that it can provide useful guidance on the transition of an organized MCS with a solid line of 50+ dbZ echoes to a more disorganized system with unsteady changes in structure and propagation. In particular, the MMP showed a noticeable decline for all MCS cases from the genesis to dissipation stages in the Northern and Southern Plains region. MMP performance in the Eastern Region was markedly poorer, however, likely because of the climatologically lower lapse rates during the summer months.

It should be noted that we are mindful of limitations of this technique and, to that end, in the use of cold pool/shear concepts for the forecasting of MCSs in general. We emphasize that the concepts presented in this paper will likely work best on MCSs that develop and continually generate strong cold pools away from strong larger-scale forcing when the shear and mean winds are substantial. However, MCSs can maintain coherence through other means, including discrete propagation along a surging outflow (one such case occurred with an MCS on 30 June 2005 in the Ohio Valley), frontogenetic circulations, low-level jet processes, gravity-wave interactions, and other larger-scale forcing mechanisms, in which the probability equations may not be as applicable.

Despite these limitations, the concepts presented above illustrate that forecast tools based on environmental variables and their statistical relationships still have the potential to provide forecasters with improved guidance on the qualitative characteristics of MCS structure and longevity. We urge the meteorological community to continue to undertake studies of this type to help improve mesoscale convective weather forecasting in the near term while we move forward into the era of convective-scale numerical weather prediction.

6. ACKNOWLEDGMENTS

This paper was greatly improved by comments from Chris Davis and an anonymous reviewer. We also thank Matt Parker and Robert Fovell for the helpful discussions regarding the background material for this paper. The SPC/NSSL 2005 Summer Program would not have been possible without the help of David Bright and Jay Liang of the SPC. We thank the SPC forecasters, particularly Steve Corfidi, and the NSSL scientists who have volunteered their time to participate in the program. We are also grateful to Bob Johns for contributing his time and wealth of knowledge and experience to this project. The majority of this project was supported through a National Research Council Postdoctoral Award for the first author under the guidance of the second author. Funding for the latter stages of the project was provided by NOAA/Office of Oceanic and Atmospheric Research under NOAA-University of Oklahoma Cooperative Agreement #NA17RJ1227, U.S. Department of Commerce.

7. REFERENCES

Benjamin, S.G. and others, 2003: An hourly assimilation-forecast cycle: The RUC. *Mon. Wea. Rev.*, 132, 495-518.

Blanchard, D.O., 1998: Assessing the vertical distribution of convective available potential energy. *Wea. Forecasting*, 13, 870-877.

Cohen, A.E., M.C. Coniglio, S.F. Corfidi, and S.J. Taylor, 2006: Discrimination among non-severe, severe, and derecho-producing mesoscale convective systems. Preprints, *86th Amer. Meteor. Soc. Annual Meeting*, CD-Rom.

Coniglio, M.C., D.J. Stensrud and M.B. Richman, 2004: An observational study of derecho-producing convective systems. *Wea. Forecasting*, 19, 320-337.

--------, --------, and L.J. Wicker, 2006a: Effects of upper-level shear on the structure and maintenance of strong quasi-linear mesoscale convective systems. *J. Atmos. Sci.*, 63, 1231-1252.

--------, H.E. Brooks, S.F. Corfidi, and S.J. Weiss, 2006b: Forecasting the maintenance of quasi-linear mesoscale convective systems. *Wea. Forecasting*, in press.

Evans, J.S., and C.A. Doswell, 2001: Examination of derecho environments using proximity soundings. *Wea. Forecasting*, 16, 329-342.

Fovell, R. G., B. Rubin-Oster, and S. Kim, 2005: A discretely propagating nocturnal Oklahoma squall line: Observations and numerical simulations. Preprints, *22nd Conf. on Severe Local Storms*, Hyannis, MA, CD-ROM.

Fritsch J.M. and G.S. Forbes, 2001: Mesoscale convective systems. *Severe Convective Storms*, *AMS Meteor. Monogr.*, C. Doswell III, Ed., 28, Amer. Meteor. Soc., 323-357.

Gale, J.J., W.A. Gallus Jr., and K.A. Jungbluth, 2002: Toward improved prediction of mesoscale convective system dissipation. *Wea. Forecasting*, 17, 856-872.

Kain. J.S., S.J. Weiss, M.E. Baldwin, G.W. Carbin, D. Bright, J.J. Levit, and J.A. Hart, 2005: Evaluating high-resolution configurations of the WRF model that are used to forecast severe convective weather: The 2005 SPC/NSSL Spring Experiment. Preprints, *21st Conf. on Weather Analysis and Forecasting*, Amer. Meteor. Soc., Washington, D.C. paper 2A.5.

Parker, M.D., and R.H. Johnson, 2004a: Structures and dynamics of quasi-2D mesoscale convective systems. *J. Atmos. Sci.*, 61, 545-567.

--------, and --------, 2004b: Simulated convective lines with leading precipitation. Part I: Governing dynamics. *J. Atmos. Sci.*, 61, 1637-1655.

--------, and --------, 2004c: Simulated convective lines with leading precipitation. Part II: Evolution and maintenance. *J. Atmos. Sci.*, 61, 1656-1673.

Trier, S.B. and C.A. Davis, 2005: Propagating nocturnal convection within a 7-day WRF-model simulation. Preprints, *32nd Conf. on Mesoscale Processes*, Amer. Meteor. Soc., CD-ROM.

Weisman, M.L., and R. Rotunno, 2004: “A theory for strong, long-lived squall lines” revisted. *J. Atmos. Sci.*, 61, 361-382.

--------, J.B. Klemp, and R. Rotunno, 1988: Structure and evolution of numerically simulated squall lines. *J. Atmos. Sci.*, 45, 1990-2013.

Wilks, D.S., 1995: *Statistical Methods in the Atmospheric Sciences*. Academic Press, 467 pp.